Total Electron Content estimation with Reg-Est

H. Nayir,[1] F. Arikan,[2] O. Arikan,[3] and C. B. Erol[4]

[1] Total Electron Content (TEC) constitutes one of the key elements for observing the variable structure of the ionosphere. GPS provides a cost-effective alternative in TEC estimation through earth-based receivers. In this paper, one of the TEC estimation methods, namely Reg-Est, is investigated in detail in terms of its parameters and developed further to include improvements. Reg-Est estimates robust TEC using GPS measurements of 30 s time resolution. The method combines the vertical TEC computed from all the satellites in view over $10°$ horizon limit in the least squares sense through the minimization of a cost function which also includes a high pass penalty filter. Optional weighting functions and sliding window median filters are added to enrich the processing and smoothing of the data. In this study, the input to the Reg-Est is enlarged to include phase-corrected TEC. The best way of including the instrumental biases is investigated and the algorithm is updated to include the biases in the slant TEC computation. The effect of the thin shell height of the ionosphere in Reg-Est estimates is studied. It is concluded that the Reg-Est algorithm is very robust to the choice of thin shell height. The best weighting function to reduce the multipath effects and to minimize the non-ionospheric noise is selected. The improved Reg-Est algorithm can be used for all latitudes and for both quite and disturbed days of the ionosphere. The Reg-Est TEC are in excellent accordance with the estimates from IGS analysis centers.

1. Introduction

[2] Ionosphere is the layer of the atmosphere that has high electron concentration, extending, roughly, from 60 km to 1000 km above Earth surface. The ionosphere presents a medium which is anisotropic, inhomogeneous, time and space variant and it can also be nonlinear at times [*Budden*, 1985; *Hargreaves*, 1992]. Short time random variations and long time periodic variations (like day-night periodicity) cause fading, distortion and dispersion of both High Frequency (HF) and satellite communication signals. The ionospheric conditions are especially severe for high latitude and equatorial regions. With its randomly variant structure both in space and time, ionosphere plays a key role in space weather. Therefore the characterization of the ionospheric variability plays an important role both in ionospheric physics and in HF and satellite communications. A well accepted approach in the investigation of spatial and temporal structure and variability of the ionosphere is the estimation of Total Electron Content (TEC) [*Lanyi and Roth*, 1988; *Komjathy and Langley*, 1996; *Schaer*, 1999; *Otsuka et al.*, 2002]. TEC is defined as the line integral of electron density along a raypath L or as a measure of the total number of electrons along a path of the radio wave

$$\text{TEC} = \int_L N_e(l)dl \qquad (1)$$

where N_e is the electron density distribution [*Budden*, 1985]. TEC can be interpreted as the number of free electrons along the raypath above one square meter on the ionosphere. The unit of TEC is TECU where 1 TECU = 10^{16} el/m². Because of the high variability of the ionosphere in space and time, the electron density distribution and TEC can be regarded as spatiotemporal random functions similar to their counterparts in geostatistics, hydrology, meteorology and environmental sciences. Characterization of TEC leads to detailed investigation and analysis of electron density distribution of the ionosphere and plays a key role in near Earth space science and space weather such as in TEC Mapping and Computerized Ionospheric Tomography [*Lanyi and Roth*, 1988; *Jakowski et al.*, 1996; *Komjathy and Langley*, 1996; *Liao*, 2000; *Otsuka et al.*, 2002; *Arikan et al.*, 2003; *Kunitsyn and Tereshchenko*, 2003].

[3] In terms of measurements, TEC is a derived quantity and can be computed from vertical ionosondes both bottom-side and top-side [*Hargreaves*, 1992], Faraday Rotation of

[1]Department of Microwave and System Technologies, Aselsan Inc., Yenimahalle, Ankara, Turkey.
[2]Department of Electrical and Electronics Engineering, Hacettepe University, Beytepe, Ankara, Turkey.
[3]Department of Electrical and Electronics Engineering, Bilkent University, Bilkent, Ankara, Turkey.
[4]TUBITAK, UEKAE, Kavaklidere, Ankara, Turkey.

satellite signals such as GLONASS and EISCAT [*Jakowski et al.*, 1996], TOPEX/POSEIDON double frequency altimeters [*Komjathy*, 1997], GPS phase and delay recordings and incoherent backscatter radar signals [*Komjathy*, 1997; *Liao*, 2000]. Yet, these measurements have very different integration paths and thus, it is very difficult to compare the computations with one another. In recent years, Global Positioning System (GPS) dual frequency signals have been widely used to estimate both regional and global TEC values [*Komjathy*, 1997; *Liao*, 2000]. The advantages of GPS signals include the large number of GPS satellites at an altitude of 20,000 km, their global coverage and commercially available receivers. Since the frequencies that are used in the GPS system are sufficiently high, the signals are minimally affected by the ionospheric absorption and the Earth's magnetic field. TEC can be derived from the delay of the traveling time of the transmitted GPS signals, recorded at the Earth-based receivers.

[4] The receivers at GPS stations record signals transmitted at two L-band frequencies namely, f_1 at 1575.42 MHz, and f_2 at 1227.60 MHz. The time delay which occurs while these signals are propagating through the ionosphere are converted to 'pseudo-ranges' and recorded as P_1 and P_2 signals. The carrier phase delay measurements on the f_1 and f_2 coherent frequencies are also recorded as L_1 and L_2, respectively [*Leick*, 2004]. TEC values can be calculated from the difference of P_2 and P_1 signals which is called the 'absolute TEC'; the difference of L_1 and L_2 can be used to compute TEC which is called as 'relative TEC'; and it is possible to compute TEC by fitting $(L_1 - L_2)$ to $(P_2 - P_1)$ measurements and also solving for instrumental biases [*Jakowski et al.*, 1996]. The TEC computation methods and their advantages and disadvantages are widely discussed in the literature [*Jakowski et al.*, 1996; *Liao*, 2000; *Arikan et al.*, 2003]. The computation of TEC from the difference of pseudo-ranges is very simple, unambiguous and does not require complicated preprocessing on data. Yet, absolute TEC computation is usually corrupted by noise and multipath signals. Although low-noise, the computation of relative TEC is complicated due to the fact that the phase delay measurements suffer from cycle ambiguities. There are various inversion procedures for fitting $(L_1 - L_2)$ to $(P_2 - P_1)$ and solving for instrumental biases such as *Lanyi and Roth* [1988] and *Ma and Maruyama* [2003]. These methods try to combine the advantages of absolute and relative TEC and thus obtain an unambiguous and low-noise TEC. Yet, all of these methods suffer from the problem of cycle slip which occurs when the GPS receiver loses the lock with the satellite signals, especially at low elevation angles and causing discontinuity in the data set [*Arikan et al.*, 2003]. The interfrequency biases which produce the instrumental biases are another important issue that needs to be handled in the computation of TEC.

[5] The standard procedure to compute TEC on the slant raypath (*STEC*) from the satellite to the receiver is provided in various studies in the literature including *Jakowski et al.* [1996], *Liao* [2000], and *Arikan et al.* [2003]. According to this procedure, *STEC* values are calculated from $(P_2 - P_1)$ or from $(L_1 - L_2)$. A combination of pseudo-range and carrier phase can be used for TEC computation such as those given by *Komjathy and Langley* [1996], *Lanyi and Roth* [1988], and *Otsuka et al.* [2002]. Since the inversion

of TEC is accomplished with different methods in the literature, the calculated TEC from various centers differ in the estimates. Most of the estimation procedures for TEC provided in the literature assume both the spatial homogeneity of ionosphere for a wide range of elevation and azimuth angles and a temporal stationarity period of at least 5 to 15 min [*Komjathy and Langley*, 1996; *Arikan et al.*, 2003]. In fact, since the ionosphere is spatially inhomogeneous and time varying, the computed STEC have different characteristics for each satellite path. Generally, in order to avoid missing and inaccurate data, most of the methods that estimate TEC from GPS data follow one satellite which is above a certain elevation angle for limited time periods. Most global and regional TEC mapping centers obtain the TEC as averages for every two-hour periods [*Arikan et al.*, 2003]. This way some of the important spatial and temporal variations over the receiving station may be missed or not observed at all.

[6] Regularized Estimation of TEC (Reg-Est) is a technique for estimation of high resolution, reliable and robust TEC estimation as discussed in detail by *Arikan et al.* [2003, 2004, 2007]. In Reg-Est, the initial step is to compute the STEC values from all available satellites above $10°$ horizon limit every 30 s for a desired GPS station. The P_1, P_2, L_1 and L_2 values and the satellite and receiver bias pairs, the satellite ephemeris data files are obtained from the IONosphere Map EXchange Format (IONEX) files from International GPS Service for Geodynamics (IGS) centers (ftp://cddisa.gsfc.nasa.gov/gps/products/ionex/). These files are preprocessed to compute STEC and then VTEC for each satellite and receiver pair every 30 s. Yet, as shown by *Arikan et al.* [2003], these computed VTEC values can have very different characteristics and they have discontinuities due to satellite paths in view with respect to receiver position. Reg-Est combines all these preprocessed signals, from all the satellites above $10°$ horizon limit and every 30 s, in the least squares sense to estimate the vertical TEC (*VTEC*) for a desired time period. VTEC estimated by the Reg-Est does not depend on one satellite or the other but rather represents the least squares sense the combination of all the information from all the satellites in view. This feature of estimating 30 s VTEC using all the satellites in view for any desired time period is unique to Reg-Est. Reg-Est reduces the contamination due to multipath by applying a weighting function on the computed TEC data according to the satellite positions with respect to the local zenith. A two step regularization algorithm combines the computed and weighted *VTEC* and provides smooth TEC estimates for the desired time period within a day with 30 s time resolution. The first step of the regularization includes the minimization of error utilizing a high pass penalty function. This step requires the determination of two regularization parameters which are chosen from the minimization of error between the the estimated and actual *VTEC* values. The second step of regularization includes a sliding window median filter which further reduces the jagged features in the estimated *VTEC*. As given in detail by *Arikan et al.* [2003, 2004, 2007], Reg-Est TEC estimates have been computed for a wide range of ionospheric states and GPS receiver stations. It is observed that Reg-Est produces high resolution, robust and reliable TEC estimates for high-latitude, mid-latitude and equatorial regions and for both

Table 1. The List of Select GPS Receiver Stations and Their Geographic Coordinates

Receiver Station	Station ID	Latitude	Longitude	Region
Ankara, Turkey	Ankr	39.53° N	32.45° E	Mid-latitude
Graz, Austria	Graz	47.04° N	15.29° E	Mid-latitude
Zelenchukskaya, Russia	Zeck	43.17° N	41.33° E	Mid-latitude
Arti, Russia	Artu	56.25° N	58.33° E	High-latitude
Kiruna, Sweden	Kiru	67.51° N	20.58° E	High-latitude
Metsahovi, Finland	Mets	60.13° N	24.41° E	High-latitude
Petropavlovsk, Russia	Petp	53.04° N	158.36° E	High-latitude
Lae, Papua New Guinea	Lae1	6.40° S	146.59° E	Equatorial
Manila, Philippines	Pimo	14.38° N	121.04° E	Equatorial
Nanyang, Singapore	Ntus	1.20° N	103.40° E	Equatorial

quiet and disturbed days of ionosphere. When compared with the TEC estimates of IGS analysis centers and International Reference Ionosphere (IRI) 2001 [*Bilitza*, 2001], very good accordance is observed, especially with the estimates of Center for Orbit Determination in Europe (CODE) and Jet Propulsion Laboratory (JPL) [*Arikan et al.*, 2003, 2007; *Nayir*, 2007]. IGS centers produce global TEC maps every two hours, whereas Reg-Est has time resolution of 30 s and TEC is computed for one station. This way Reg-Est has better space and time resolution when compared to other estimates. Many ionospheric disturbances and effects of geomagnetic storms can better be observed with such a time and space resolution. Reg-Est produces robust estimates with the same parameter set both for highly disturbed days and quiet days and also for all regions of ionosphere. Reg-Est estimates represent the actual recordings of GPS receivers whereas JPL and CODE smooth the values with methods only very generally known to the public. Therefore Reg-Est TEC since it does not contain any smoothing or averaging in time or space, is better in representing the actual ionospheric situation. This is a very important aspect in monitoring the space weather and in ionospheric tomography. The ambiguity about how the differential code biases should be included into the STEC computation is resolved in Reg-Est preprocessing of recorded GPS observables.

[7] In this study, some important parameters that are used in Reg-Est method such as ionospheric thin shell height, weighting function, inclusion of instrumental biases are investigated in detail. The robustness of Reg-Est with respect to the choice of ionospheric height, the optimum weighting function which best reduces the non-ionospheric noise effects and alternative methods for using satellite and receiver instrumental biases are analyzed. A basic solution to fitting pseudo-range to phase delay data is also suggested. The Reg-Est is applied to the quiet days, positively and negatively disturbed days of October 2003 and April 2001 according to the list provided by Ionospheric Dispatch Center in Europe (IDCE) (http://www.cbk.waw.pl/rwc/idce.html). According to IDCE, 10–12 October 2003 are quiet days; 27 to 29 October 2003 and 28 April 2001 are positively disturbed days; 30-31 October 2003 are negatively disturbed days. Between 27-31 October 2003, there was a severe geomagnetic storm causing major disturbance in the ionosphere. *Kp* index rose as high as 9 and *Dst* index

fell to -400 nT as given by *Arikan et al.* [2007]. A partial list of the studies for October 2003 storm includes *Foster and Rideout* [2005], *Lin et al.* [2005], *Mitchell et al.* [2005], and *Yizengaw et al.* [2005]. In this paper, Reg-Est is applied to the data from the GPS receiver stations from equatorial, mid-latitude and high-latitude stations, listed in Table 1.

[8] In section 3, the proper inclusion of the IONEX satellite and receiver bias is discussed. In section 4, computation of phase-corrected *VTEC* from individual satellites is introduced. The choice of ionospheric thin shell height is provided in section 5. Section 6 consists of the discussion on weighting the GPS measurements to reduce the multipath effects. The comparisons of Reg-Est estimates are provided with those from the analysis centers of IGS such as JPL, European Space Operations Center of European Space Agency (ESA/ESOC), CODE, Polytechnical University of Catalonia (UPC) [*Arikan et al.*, 2003].

2. Ionospheric Delay Model of Dual-Frequency GPS Signals

[9] The Earth based GPS receivers record the delayed and phase shifted signals in a special format called Receiver Independent Exchange Format (RINEX) [*Leick*, 2004]. As mentioned in section 1, the time delay of signals are converted to pseudo-range values and the phase shifts are recorded as phase delays in the receivers [*Leick*, 2004]. The standard model for pseudo-range recordings for two frequencies f_1 and f_2 are as follows:

$$P_{1,u}^m = p_u^m + c(\delta t_u - \delta t^m) + d_{trop,u}^m + d_{ion1,u}^m + c(\varepsilon_1^m + \varepsilon_{1,u}) \quad (2)$$

$$P_{2,u}^m = p_u^m + c(\delta t_u - \delta t^m) + d_{trop,u}^m + d_{ion2,u}^m + c(\varepsilon_2^m + \varepsilon_{2,u}) \quad (3)$$

where the subscript u denotes the receiver station index; the superscript m denotes the satellite index. p is the actual range between satellite and receiver, δt_u and δt^m are the clock errors for the receiver and satellite, respectively. d_{trop} and d_{ion} are the troposphere and ionosphere group delays, respectively. ε^m and ε_u are the frequency dependent satellite and receiver biases [*Leick*, 2004]. c is the speed of light in vacuum. The difference of equations (2) and (3) is called the geometry free linear combination of pseudo-range because the actual range p is eliminated as:

$$\begin{aligned} P_{4,u}^m &= P_{2,u}^m - P_{1,u}^m \\ &= d_{ion2,u}^m - d_{ion1,u}^m + c(\varepsilon_2^m - \varepsilon_1^m) + c(\varepsilon_{2,u} - \varepsilon_{1,u}) \end{aligned} \quad (4)$$

Using satellite and receiver biases for f_1 and f_2 frequency signals, differential code biases (DCBs) are defined for the satellite and receiver as follows [*Leick*, 2004]:

$$DCB^m = \varepsilon_1^m - \varepsilon_2^m \quad (5)$$

$$DCB_u = \varepsilon_{1,u} - \varepsilon_{2,u} \quad (6)$$

where DCB^m and DCB_u are the differential code biases for the satellite and receiver, respectively.

[10] Similar equations can be written for phase delay observations $L_{1,u}^m$ and $L_{2,u}^m$ as [*Leick*, 2004]:

$$L_{1,u}^m = \lambda_1 \Phi_{1,u}^m = p_u^m + c(\delta t_u - \delta t^m) + \lambda_1 \Phi_{ion1,u}^m \\ + \lambda_1 \Phi_{trop,u}^m - c(\varepsilon_1^m + \varepsilon_{1,u}) + \lambda_1 N_1^m \quad (7)$$

$$L_{2,u}^m = \lambda_2 \Phi_{2,u}^m = p_u^m + c(\delta t_u - \delta t^m) + \lambda_2 \Phi_{ion2,u}^m \\ + \lambda_2 \Phi_{trop,u}^m - c(\varepsilon_2^m + \varepsilon_{2,u}) + \lambda_2 N_2^m \quad (8)$$

where λ_1 and λ_2 are the wavelengths corresponding to f_1 and f_2 frequencies, $\Phi_{1,u}^m$ and $\Phi_{2,u}^m$ are the recorded the phase delays corresponding to f_1 and f_2 frequencies, respectively. $\Phi_{ion1,u}^m$ and $\Phi_{ion2,u}^m$ are the ionospheric phase delays corresponding to f_1 and f_2 frequencies, respectively. N_1^m and N_2^m, denote the initial phase ambiguity corresponding to f_1 and f_2 frequencies, respectively, for the mth satellite. Finally, $\Phi_{trop,u}^m$ is the phase delay due to troposphere.

[11] The difference of equations (7) and (8) is called the geometry free linear combinations of phase delay and is given as [*Leick*, 2004]:

$$L_{4,u}^m = \lambda_1 \Phi_{1,u}^m - \lambda_2 \Phi_{2,u}^m = \lambda_1 \Phi_{ion1,u}^m - \lambda_2 \Phi_{ion2,u}^m \\ + c(DCB^m) + c(DCB_u) + \Delta N^m \quad (9)$$

and ΔN^m in equation (9) is defined as

$$\Delta N^m = \lambda_1 N_1^m - \lambda_2 N_2^m \quad (10)$$

Using the approximation given by *Liao* [2000] and *Leick* [2004]:

$$d_{ion,u}^m = -\Phi_{ion,u}^m \frac{c}{f} \approx A \frac{STEC_u^m}{f^2} \quad (11)$$

where $A = 40.3$ m³/s² and $STEC_u^m$ denotes the total electron content on the slant raypath combining the receiver u and the satellite m. Using equation (11) in equations (4) and (9), the following expressions for the geometry free combinations are obtained [*Leick*, 2004; *Komjathy*, 1997; *Nayir*, 2007]:

$$P_{4,u}^m = A \left(\frac{f_1^2 - f_2^2}{f_1^2 f_2^2} \right) STEC_u^m - c(DCB^m + DCB_u) \quad (12)$$

$$L_{4,u}^m = A \left(\frac{f_1^2 - f_2^2}{f_1^2 f_2^2} \right) STEC_u^m - c(DCB^m + DCB_u) + \Delta N^m \quad (13)$$

In the following section, alternative methods of inclusion of the DCBs in the *STEC* computation.

3. Inclusion of IONEX Instrumental Biases

[12] The geometry free combinations for the pseudorange and phase delays given in the previous section can be used to estimate *STEC* values for each receiver and satellite pair. In the estimation of *STEC*, the differential code biases also need to be known. f_1 and f_2 frequency signals take different paths in satellite or receiver hardware. Therefore DCBs can be defined as differential delay of f_1 and f_2 frequency signals due to satellite or receiver hardware [*Komjathy*, 1997]. For some IGS stations and for certain dates, the DCBs are provided in the IONEX files mostly from JPL, CODE and ESA. However, there is no standard procedure on how to include these instrumental biases into the TEC computation [*Warnant*, 1997; *Makalea et al.*, 2001]. One of the most common methods is the inclusion of these biases in *STEC* computation as follows [*Komjathy*, 1997]:

$$STEC_u^m(n) = \frac{1}{A} \left(\frac{f_1^2 f_2^2}{f_1^2 - f_2^2} \right) \left[P_{4,u}^m(n) + c(DCB^m + DCB_u) \right] \quad (14)$$

where the index n denotes the time sample, and $1 \le n \le N$. N is the total number of time samples in a recording. A typical GPS receiver records the data every 30 s. Thus for a receiver that records for a continuous 24 h, N gets the value of $N = 2 \times 60 \times 24 = 2880$. The TEC in the local zenith direction at the ionospheric pierce point is known as vertical TEC (*VTEC*). The mapping function that combines *STEC* and *VTEC* can be computed done by *Lanyi and Roth* [1988], *Otsuka et al.* [2002], and *Ma and Maruyama* [2003]:

$$VTEC_u^m(n) = STEC_u^m(n)/M(\epsilon^m(n)) \quad (15)$$

where $M(\epsilon)$ is the mapping function

$$M(\epsilon^m(n)) = \left[1 - \left(\frac{R \cos \epsilon^m(n)}{R + h} \right)^2 \right]^{-1/2} \quad (16)$$

In equations (15) and (16), ϵ^m is the local elevation angle of mth satellite; h is the ionospheric thin shell height, and R is the radius of Earth. When $VTEC_u^m(n)$ of equations (14) and (15) is used as the input of Reg-Est method, the Reg-Est TEC estimates are denoted as $N \times 1$ vector, $\tilde{\mathbf{x}}_{b1}$.

[13] An alternative method in inclusion of the receiver and satellite biases at the *VTEC* computation is given by *Arikan et al.* [2003, 2004] as follows:

$$STEC_u^m(n) = \frac{1}{A} \left(\frac{f_1^2 f_2^2}{f_1^2 - f_2^2} \right) \left[P_{4,u}^m(n) \right] \quad (17)$$

$$VTEC_u^m(n) = \left(STEC_u^m(n)/M(\epsilon^m(n)) \right) + b^m + b_u \quad (18)$$

where the satellite and receiver biases b^m and b_u are in TECU (1 ns = 2.854 TECU). When equation (18) is used as input to Reg-Est, the Reg-Est TEC estimates are denoted as an $N \times 1$ vector, $\tilde{\mathbf{x}}_{b2}$.

[14] In order to compare the estimates $\tilde{\mathbf{x}}_{b1}$ (equation (15)) and $\tilde{\mathbf{x}}_{b2}$ (equation (18)) with each other and also with the estimates of JPL ($\tilde{\mathbf{x}}_{JPL}$), CODE ($\tilde{\mathbf{x}}_{CODE}$), ESA, UPC and IGS, the Reg-Est is applied to stations in Table 1 both for quiet and disturbed days of October 2003. An example of TEC estimates is given in Figure 1. In Figure 1a and in Figure 1b, both bias adding methods give consistent TEC estimation results with IGS analysis centers especially with
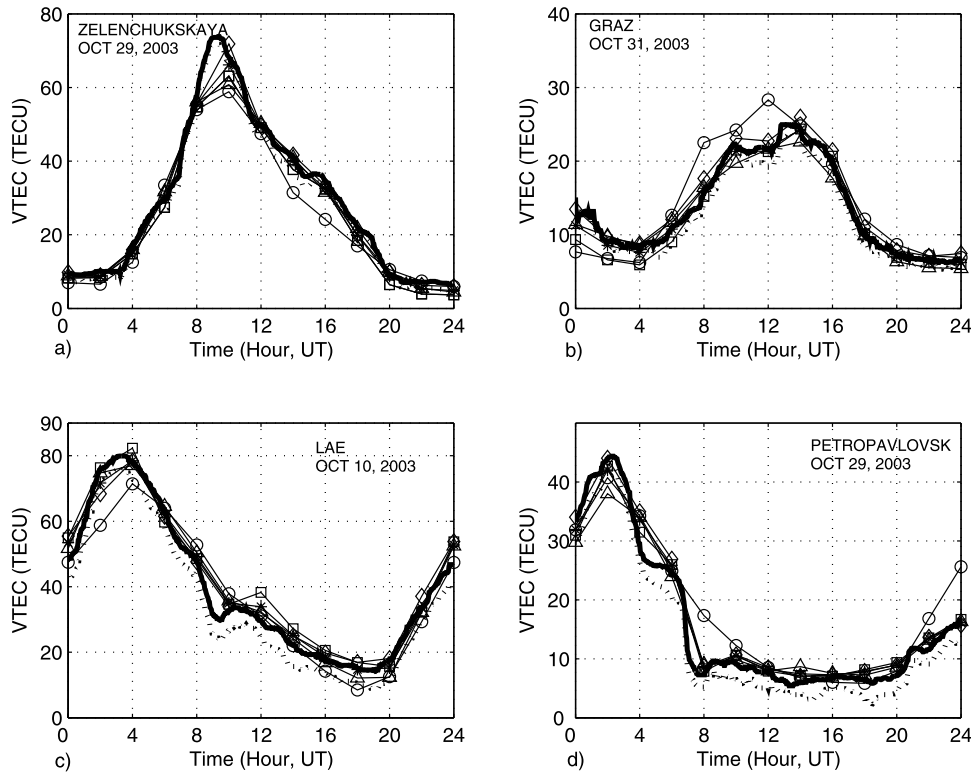
Figure 1. Incorporation of instrumental biases to Reg-Est and comparison with IGS analysis centers, $\tilde{\mathbf{x}}_{b1}$ (solid line) and $\tilde{\mathbf{x}}_{b2}$ (dashed line), JPL (diamond), CODE (square), ESA/ESOC (circle), UPC (triangle), IGS (stars). a) Zelenchukskaya, 29 October 2003 b) Graz, 31 October 2003 c) Lae, 10 October 2003 d) Petropavlovsk, 29 October 2003.

CODE and JPL. In Figure 1c and Figure 1d, $\tilde{\mathbf{x}}_{b1}$ is in better agreement with $\tilde{\mathbf{x}}_{CODE}$ and $\tilde{\mathbf{x}}_{JPL}$.

[15] The detailed comparison of $\tilde{\mathbf{x}}_{b1}$ and $\tilde{\mathbf{x}}_{b2}$ with each other and also with $\tilde{\mathbf{x}}_{JPL}$ and $\tilde{\mathbf{x}}_{CODE}$ is obtained by computing the normalized TEC differences using equation (19) through equation (23) as follows:

$$Err_1 = \frac{\sum_{n=1}^{N} |\tilde{\mathbf{x}}_{b1}(n) - \tilde{\mathbf{x}}_{b2}(n)|^2}{\sum_{n=1}^{N} |\tilde{\mathbf{x}}_{b1}(n)|^2} \qquad (19)$$

$$Err_2 = \frac{\sum_{n=1}^{N} |\tilde{\mathbf{x}}_{b1}(n) - \tilde{\mathbf{x}}_{JPL}(n)|^2}{\sum_{n=1}^{N} |\tilde{\mathbf{x}}_{b1}(n)|^2} \qquad (20)$$

$$Err_3 = \frac{\sum_{n=1}^{N} |\tilde{\mathbf{x}}_{b1}(n) - \tilde{\mathbf{x}}_{CODE}(n)|^2}{\sum_{n=1}^{N} |\tilde{\mathbf{x}}_{b1}(n)|^2} \qquad (21)$$

$$Err_4 = \frac{\sum_{n=1}^{N} |\tilde{\mathbf{x}}_{b2}(n) - \tilde{\mathbf{x}}_{JPL}(n)|^2}{\sum_{n=1}^{N} |\tilde{\mathbf{x}}_{b2}(n)|^2} \qquad (22)$$

$$Err_5 = \frac{\sum_{n=1}^{N} |\tilde{\mathbf{x}}_{b2}(n) - \tilde{\mathbf{x}}_{CODE}(n)|^2}{\sum_{n=1}^{N} |\tilde{\mathbf{x}}_{b2}(n)|^2} \qquad (23)$$

In the above equations n denotes the time index of the vectors and N is the total number of estimations. The normalized TEC differences are provided in Table 2 various receiver stations and for both quiet and disturbed days. As is

observed from Table 2, Err_1 indicates that $\tilde{\mathbf{x}}_{b1}$ and $\tilde{\mathbf{x}}_{b2}$ are in very good agreement. When Err_1 is compared with Err_4 and Err_3 is compared to Err_5, $\tilde{\mathbf{x}}_{b1}$ is in better agreement with those of JPL and CODE. Thus in further use of Reg-Est, the instrumental biases will be included in the $STEC$ computation as in equation (14).

4. Carrier Phase-Corrected TEC Estimation

[16] The Reg-Est method developed by *Arikan et al.* [2003, 2004] inputs $VTEC_u^m(n)$ with sampling period of 30 s from all the satellites in view. $VTEC$ for each satellite and any time instant can be computed from the pseudo-range and phase measurements recorded by the GPS receiver in Receiver Independent Exchange Format (RINEX) as explained in detail in the previous sections. In order to combine the advantages of both pseudo-range and phase recordings in $STEC$ and $VTEC$ computations, the L_4 data are usually fitted to the P_4 by various algorithms in the literature as *Jakowski et al.* [1996], *Komjathy and Langley* [1996], *Lanyi and Roth* [1988], and *Otsuka et al.* [2002]. In this study, the phase-corrected or phase-leveled TEC computation is implemented and the input range of Reg-Est is extended to include less noisy phase measurements. The leveling or fitting of L_4 to P_4 is usually accomplished by defining a baseline for each connected arc of phase measurements as [*Lanyi and Roth*, 1988; *Otsuka et al.*, 2002]:

$$B^m = \frac{1}{N_{me}} \sum_{n_{me}=1}^{N_{me}} \left(P_{4,u}^m(n_{me}) - L_{4,u}^m(n_{me}) \right) \qquad (24)$$

Table 2. Normalized TEC Differences for Using Different Bias Methods for Reg-Est and Comparison With CODE and JPL Estimates

| Station ID	Day	Err_1	Err_2	Err_3	Err_4	Err_5
Graz	10 October 2003	8.98×10^{-3}	3.20×10^{-2}	2.19×10^{-3}	1.07×10^{-1}	2.87×10^{-2}
Artu	10 October 2003	6.72×10^{-2}	4.53×10^{-2}	4.21×10^{-3}	4.04×10^{-1}	9.80×10^{-2}
Lae1	10 October 2003	1.36×10^{-2}	6.42×10^{-3}	8.61×10^{-3}	3.63×10^{-2}	4.41×10^{-2}
Zeck	12 October 2003	1.17×10^{-2}	9.04×10^{-3}	2.85×10^{-3}	4.05×10^{-2}	1.48×10^{-2}
Petp	12 October 2003	3.54×10^{-2}	5.35×10^{-2}	3.14×10^{-3}	2.43×10^{-1}	4.56×10^{-2}
Ntus	12 October 2003	1.27×10^{-4}	3.77×10^{-3}	5.12×10^{-3}	3.65×10^{-3}	5.27×10^{-3}
Lae1	28 October 2003	8.94×10^{-3}	6.03×10^{-3}	3.53×10^{-2}	2.15×10^{-2}	7.23×10^{-2}
Zeck	29 October 2003	3.16×10^{-3}	1.99×10^{-3}	6.87×10^{-3}	6.04×10^{-3}	1.82×10^{-3}
Petp	29 October 2003	1.81×10^{-2}	1.01×10^{-2}	5.98×10^{-3}	5.89×10^{-2}	4.17×10^{-2}
Artu	30 October 2003	7.99×10^{-2}	2.05×10^{-2}	1.68×10^{-2}	3.11×10^{-1}	1.43×10^{-1}
Ntus	30 October 2003	6.78×10^{-4}	2.90×10^{-3}	9.00×10^{-3}	1.95×10^{-2}	7.25×10^{-3}
Graz	31 October 2003	8.71×10^{-3}	6.59×10^{-3}	1.73×10^{-2}	3.22×10^{-2}	2.03×10^{-2}

where B^m denotes the leveling baseline value for the mth satellite for the time duration of a total of N_{me} samples in each phase connected arc. n_{me} is the time index of the samples in the connected phase arc. The leveling baseline value B^m is combined with the P_4 in equation (14) to yield the slant TEC as follows:

$$STEC_u^m(n) = \frac{1}{A}\left(\frac{f_1^2 f_2^2}{f_1^2 - f_2^2}\right)\left(B^m + L_{4,u}^m(n) + c(DCB_u + DCB^m)\right)$$

(25)

Thus $STEC$ can be computed from equations (14) or (25) and either data set can be used as input to the Reg-Est algorithm. The vertical TEC can be computed from $STEC$ as in equation (15).

[17] In the following discussion, the Reg-Est TEC estimates which are obtained from equations (14) and (15) will be called $\tilde{\mathbf{x}}_{pr}$. The Reg-Est TEC estimates which are obtained from equations (25) and (15) will be called $\tilde{\mathbf{x}}_{ph}$. The $\tilde{\mathbf{x}}_{pr}$ and $\tilde{\mathbf{x}}_{ph}$ are compared with TEC estimates from the IONEX files from IGS centers and an example plot is provided in Figure 2. In Figure 2, the solid line denotes $\tilde{\mathbf{x}}_{ph}$ and the dashed line denote $\tilde{\mathbf{x}}_{pr}$. It is observed for the stations and for both quiet and disturbed days of October 2003 given in Table 1, Reg-Est algorithm is very robust with respect to noisy inputs. As can be seen from the example in Figure 2, both $\tilde{\mathbf{x}}_{pr}$ and $\tilde{\mathbf{x}}_{ph}$ are very close to each other and they are both in very good agreement with the estimates of IGS centers, especially with JPL and CODE.

[18] In order to compare the differences of $\tilde{\mathbf{x}}_{pr}$ and $\tilde{\mathbf{x}}_{ph}$ with respect to the best fitting IONEX estimates, CODE and
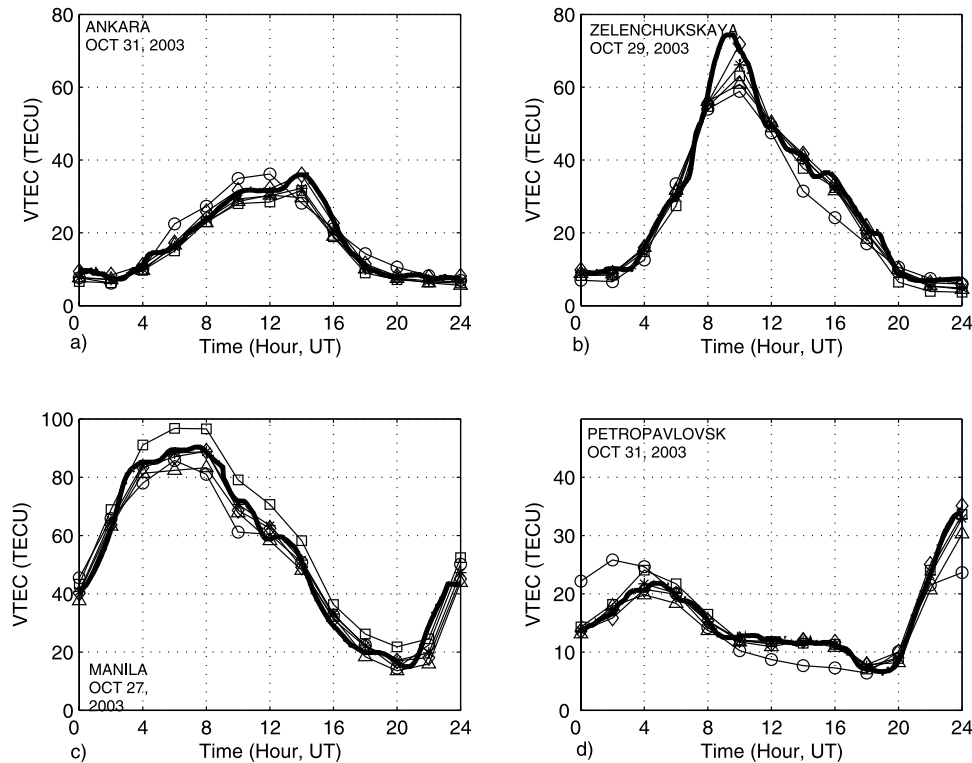
Figure 2. Comparison of Reg-Est TEC estimates $\tilde{\mathbf{x}}_{pr}$ (dashed line) and $\tilde{\mathbf{x}}_{ph}$ (solid line) with estimates from JPL (diamond), CODE (square), ESA/ESOC (circle), UPC (triangle), IGS (stars). a) Ankara, 31 October 2003 b) Zelenchukskaya, 29 October 2003 c) Manila, 27 October 2003 d) Petropavlovsk, 31 October 2003.

Table 3. Normalized TEC Differences When $\tilde{\mathbf{x}}_{pr}$ and $\tilde{\mathbf{x}}_{ph}$ are Compared With $\tilde{\mathbf{x}}_{CODE}$ and $\tilde{\mathbf{x}}_{JPL}$ in Equations (26) to (30)

Station ID	Day	Err_6	Err_7	Err_8	Err_9	Err_{10}
Graz	10 October 2003	8.20×10^{-4}	3.20×10^{-2}	2.19×10^{-3}	3.21×10^{-2}	1.67×10^{-3}
Artu	10 October 2003	2.29×10^{-3}	4.53×10^{-2}	4.21×10^{-3}	4.59×10^{-2}	5.12×10^{-3}
Lae1	10 October 2003	1.89×10^{-4}	6.42×10^{-3}	8.61×10^{-3}	7.68×10^{-3}	1.06×10^{-2}
Pimo	27 October 2003	2.38×10^{-5}	4.05×10^{-3}	1.53×10^{-2}	3.84×10^{-3}	1.54×10^{-2}
Zeck	29 October 2003	2.68×10^{-4}	1.99×10^{-3}	6.87×10^{-3}	1.49×10^{-3}	8.63×10^{-3}
Ntus	30 October 2003	4.94×10^{-4}	2.90×10^{-3}	9.00×10^{-3}	3.36×10^{-3}	9.81×10^{-3}
Petp	31 October 2003	5.07×10^{-4}	2.87×10^{-3}	5.40×10^{-3}	2.68×10^{-3}	5.80×10^{-3}
Ankr	31 October 2003	1.75×10^{-4}	1.30×10^{-3}	1.56×10^{-2}	1.93×10^{-3}	1.60×10^{-2}

JPL, a set of normalized differences are calculated for all the stations in Table 1 and for both quiet and disturbed days of October 2003 as follows:

$$Err_6 = \frac{\sum_{n=1}^{N} |\tilde{\mathbf{x}}_{pr}(n) - \tilde{\mathbf{x}}_{ph}(n)|^2}{\sum_{n=1}^{N} |\tilde{\mathbf{x}}_{pr}(n)|^2} \qquad (26)$$

$$Err_7 = \frac{\sum_{n=1}^{N} |\tilde{\mathbf{x}}_{pr}(n) - \tilde{\mathbf{x}}_{JPL}(n)|^2}{\sum_{n=1}^{N} |\tilde{\mathbf{x}}_{pr}(n)|^2} \qquad (27)$$

$$Err_8 = \frac{\sum_{n=1}^{N} |\tilde{\mathbf{x}}_{pr}(n) - \tilde{\mathbf{x}}_{CODE}(n)|^2}{\sum_{n=1}^{N} |\tilde{\mathbf{x}}_{pr}(n)|^2} \qquad (28)$$

$$Err_9 = \frac{\sum_{n=1}^{N} |\tilde{\mathbf{x}}_{ph}(n) - \tilde{\mathbf{x}}_{JPL}(n)|^2}{\sum_{n=1}^{N} |\tilde{\mathbf{x}}_{ph}(n)|^2} \qquad (29)$$

$$Err_{10} = \frac{\sum_{n=1}^{N} |\tilde{\mathbf{x}}_{ph}(n) - \tilde{\mathbf{x}}_{CODE}(n)|^2}{\sum_{n=1}^{N} |\tilde{\mathbf{x}}_{ph}(n)|^2} \qquad (30)$$

where n denotes the time index of the vectors and N is the total number of estimates. An example of the normalized differences are given in Table 3. As can be observed from Table 3, for all the stations and for both quiet and disturbed days, the normalized differences of Err_6 is very small and thus Reg-Est estimates TEC both from high or low noise inputs with the same reliability. When $\tilde{\mathbf{x}}_{pr}$ and $\tilde{\mathbf{x}}_{ph}$ are compared with $\tilde{\mathbf{x}}_{CODE}$ and $\tilde{\mathbf{x}}_{JPL}$, it is observed that there is excellent agreement with the two-hourly estimates of JPL and CODE.

5. The Choice of Ionospheric Thin Shell Height

[19] Many TEC estimation techniques in the literature use the Single Layer Ionosphere Model (SLIM) such as *Lanyi and Roth* [1988], *Schaer* [1999], *Otsuka et al.* [2002], and *Arikan et al.* [2003]. In SLIM model, ionosphere is assumed to be a thin, spherical shell of constant ionospheric height. This height generally corresponds to the height of maximum ionization density. SLIM model enables a conversion between *STEC* and *VTEC* using equation (15). In literature, ionospheric heights from 300 km to 450 km have been used due to varying height of maximum ionization density. In the study of *Komjathy* [1997], ionospheric shell heights of 300 km, 350 km and 400 km are used in TEC estimation procedure and TEC differences are investigated for certain mid-latitude stations. *Schaer* [1999] compared the SLIM function and Chapman profile for different ionospheric heights and ionospheric height of 428.8 km is stated to

give the best fit with Chapman Profile. The IGS-GIM model uses ionospheric height of 450 km [*Feltens and Jakowski*, 2002]. *Manucci et al.* [1998] also selects the ionospheric height as 450 km since this height is the median value of daytime ionization. Ionospheric height can be an important parameter for TEC estimation in some models. Using different ionospheric heights can result in TEC differences at 2 TECU level [*Komjathy and Langley*, 1996].

[20] Thin shell height enters the TEC estimation in conversion from *STEC* to *VTEC* in equation (15) through the mapping function $M(\epsilon^m)$ in equation (16). Reg-Est inputs the $VTEC_u^m(n)$, for the uth receiver and mth satellite, where in the mapping function in equation (16), various thin shell heights h might have been used. In order to study the effect of ionospheric height to the performance of TEC estimates, Reg-Est is carried out for ionospheric heights of $h1 = 300$ km, $h2 = 428.8$ km, and $h3 = 450$ km. In Figure 3, an example of TEC estimates of Reg-Est method for mid-latitude, high latitude and equatorial stations and both quiet and disturbed days of ionosphere are given for the ionospheric heights $h1$, $h2$, and $h3$. It is observed that the Reg-Est is a robust estimation method in terms of choosing the correct ionospheric shell height. The differences between the estimates are negligibly small. In order to observe the details between the estimates, the absolute differences between the estimates are calculated as follows:

$$Err_{11}(n) = |\tilde{\mathbf{x}}_{h2}(n) - \tilde{\mathbf{x}}_{h1}(n)| \qquad (31)$$

$$Err_{12}(n) = |\tilde{\mathbf{x}}_{h3}(n) - \tilde{\mathbf{x}}_{h2}(n)| \qquad (32)$$

Err_{11} corresponds to the absolute differences between the regularized TEC estimates $\tilde{\mathbf{x}}_{h2}$ and $\tilde{\mathbf{x}}_{h1}$ when the thin shell heights $h2$ and $h1$ are used, respectively. Similarly, Err_{12} corresponds to the absolute differences between the regularized TEC estimates $\tilde{\mathbf{x}}_{h3}$ and $\tilde{\mathbf{x}}_{h2}$ when the thin shell heights $h3$ and $h2$ are used, respectively. The absolute differences are computed for all the stations in Table 1 and for both quiet and disturbed days of October 2003. An example plot for Err_{11} and Err_{12} is given in Figure 4. As can also be observed from this figure, all the absolute TEC estimate differences are below 1 TECU. The mean of absolute differences Err_{13} and Err_{14} are also calculated in equations (33) and (34), respectively.

$$Err_{13} = \frac{1}{N} \sum_{n=1}^{N} |\tilde{\mathbf{x}}_{h2}(n) - \tilde{\mathbf{x}}_{h1}(n)| \qquad (33)$$

$$Err_{14} = \frac{1}{N} \sum_{n=1}^{N} |\tilde{\mathbf{x}}_{h3}(n) - \tilde{\mathbf{x}}_{h2}(n)| \qquad (34)$$
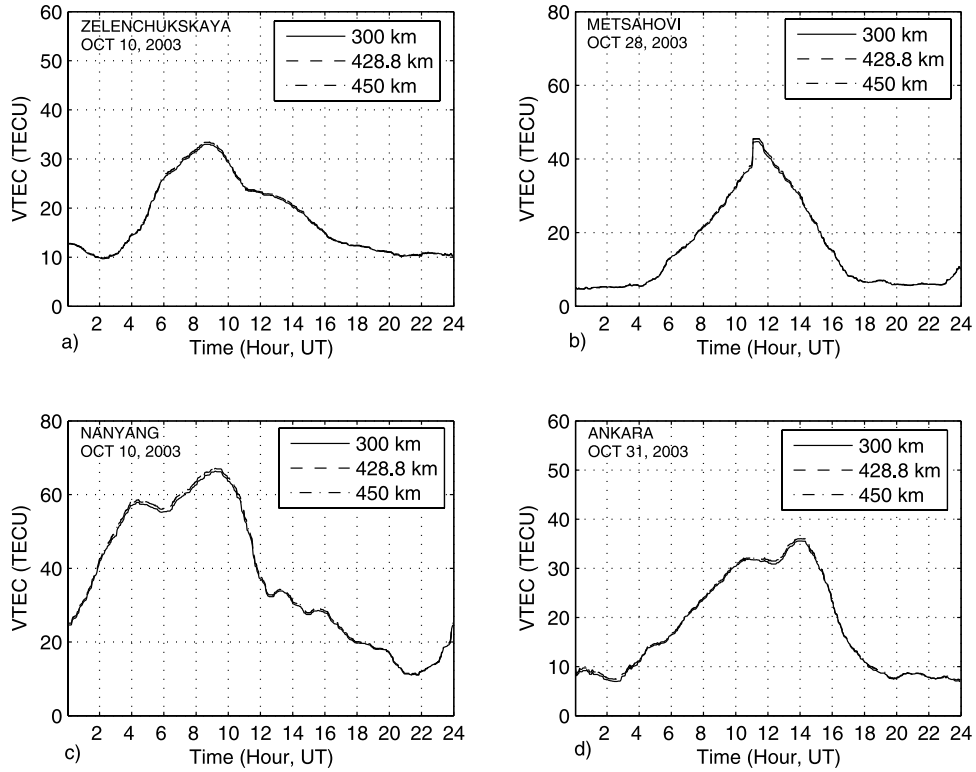
Figure 3. Reg-Est TEC estimates $\tilde{\mathbf{x}}_{h1}$, $\tilde{\mathbf{x}}_{h2}$ and $\tilde{\mathbf{x}}_{h3}$ corresponding to 300 km (solid Line), 428.8 km (dashed line), 450 km (dashed and dotted line), respectively. a) Zelenchukskaya, 10 October 2003 b) Metsahovi, 28 October 2003 c) Nanyang, 10 October 2003 d) Ankara, 31 October 2003.
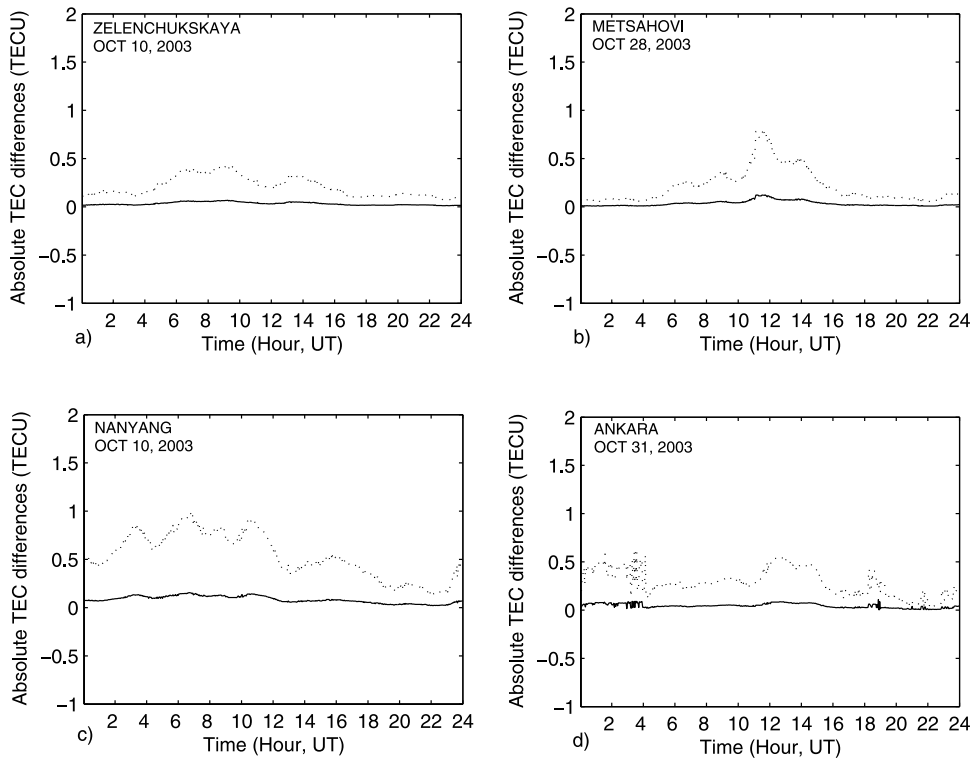
Figure 4. Absolute differences of Reg-Est TEC estimates for different ionospheric heights, Err_{11} (dotted Line), Err_{12} (solid line). a) Zelenchukskaya, 10 October 2003 b) Metsahovi, 28 October 2003 c) Nanyang, 10 October 2003 d) Ankara, 31 October 2003.

Table 4. Mean Differences Between TEC Estimates for Various Ionospheric Heights

Station ID	Day	Err_{13} (TECU)	Err_{14} (TECU)
Zeck	10 October 2003	0.207	0.032
Ntus	10 October 2003	0.534	0.083
Mets	28 October 2003	0.214	0.033
Ank	31 October 2003	0.286	0.044

where n denotes the time index of the vectors and N is the total number of estimates. The mean differences Err_{13} and Err_{14} corresponding to the stations and days given in Figure 4 are provided in Table 4. In Table 4, the largest mean difference of TEC estimates from Reg-Est is 0.534 TECU. For mid-latitude stations, this difference is below 0.3 TECU, corresponding to 1 ns of ionosphere delay. Thus Reg-Est method produces TEC estimates which are practically independent of the choice of ionospheric height. This robustness consists of one of the strongest and most important aspects of Reg-Est.

6. Weighting GPS Measurements

[21] Another parameter used in Reg-Est method is the weighting function. The measurements of satellites that are at low elevation angles are prone to multipath effects. Thus various TEC estimation methods in the literature have methods for weighting the measurements with respect to the local elevation angles. *Manucci et al.* [1998] used a 10° elevation angle limit. *Makalea et al.* [2001] uses 25° elevation angle limit. *Otsuka et al.* [2002] does not use measurements below 30° elevation limit and the weighting function depends on the slant factor. *Ma and Maruyama*

[2003] uses $\sin^2(\epsilon^m)$ as a weighting function. The weighting function used in Reg-Est is given below

$$w1^m(n) = \begin{cases} 1, & 60° \leq \epsilon^m(n) \leq 90° \\ \exp\left(-(90 - \epsilon^m(n))^2/2\sigma^2\right), & 10° < \epsilon^m(n) < 60° \\ 0, & \epsilon^m(n) < 10° \end{cases} \quad (35)$$

An optional weighting function can be suggested as:

$$w2^m(n) = \begin{cases} 1, & 60° \leq \epsilon^m(n) \leq 90° \\ \exp\left(-(60 - \epsilon^m(n))^2/2\sigma^2\right), & 10° < \epsilon^m(n) < 60° \\ 0, & \epsilon^m(n) < 10° \end{cases} \quad (36)$$

where $w2^m$ is smoother than $w1^m$ in the sense that the mean of the Normal distribution is at 60°. Equation (37) is the weighting function used by *Ma and Maruyama* [2003].

$$w3^m(n) = \sin^2(\epsilon^m(n)) \quad (37)$$

The weighting functions given in equations (35), (36) and (37) are used in Reg-Est separately giving TEC estimates $\tilde{\mathbf{x}}_{w1}$, $\tilde{\mathbf{x}}_{w2}$, and $\tilde{\mathbf{x}}_{w3}$, respectively for the GPS stations given in Table 1, for the quiet and disturbed days of October 2003. An example plot of TEC estimates $\tilde{\mathbf{x}}_{w1}$, $\tilde{\mathbf{x}}_{w2}$, and $\tilde{\mathbf{x}}_{w3}$ is provided in Figure 5. It is observed that $\tilde{\mathbf{x}}_{w2}$ and $\tilde{\mathbf{x}}_{w3}$ are
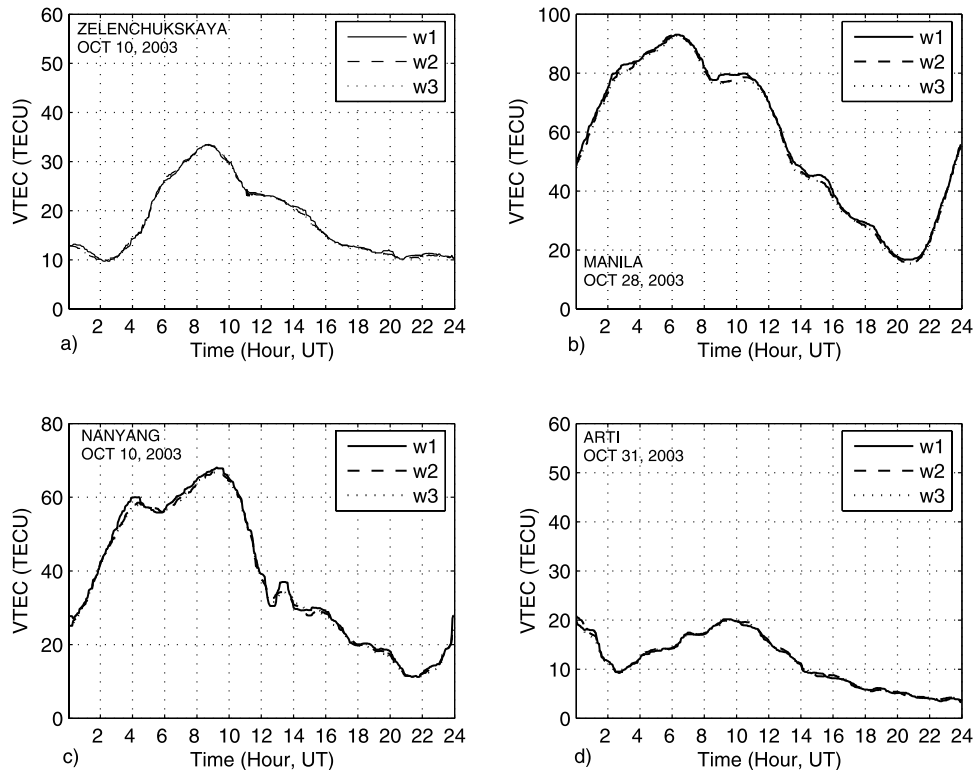
Figure 5. Reg-Est TEC, $\tilde{\mathbf{x}}_{w1}$, $\tilde{\mathbf{x}}_{w2}$ and $\tilde{\mathbf{x}}_{w3}$. a) Zelenchukskaya, 10 October 2003 b) Manila, 28 October 2003 c) Nanyang, 10 October 2003 d) Arti, 31 October 2003.

Table 5. Normalized Reg-Est TEC Differences by Using Weighting Functions, $w1^m(n)$, $w2^m(n)$, and $w3^m(n)$

Station ID	Day	Err_{15}	Err_{16}	Err_{17}
Zeck	10 October 2003	8.69×10^{-5}	4.03×10^{-4}	4.34×10^{-4}
Ankr	10 October 2003	9.51×10^{-5}	2.34×10^{-4}	3.06×10^{-4}
Mets	10 October 2003	1.53×10^{-4}	5.06×10^{-4}	5.95×10^{-4}
Artu	10 October 2003	7.77×10^{-5}	4.09×10^{-4}	3.42×10^{-4}
Pimo	10 October 2003	2.53×10^{-4}	5.94×10^{-4}	1.10×10^{-3}
Ntus	10 October 2003	1.71×10^{-4}	7.39×10^{-4}	9.41×10^{-4}
Zeck	28 October 2003	5.14×10^{-5}	1.92×10^{-4}	1.68×10^{-4}
Mets	28 October 2003	1.62×10^{-4}	3.04×10^{-4}	5.20×10^{-4}
Pimo	28 October 2003	9.66×10^{-5}	3.58×10^{-4}	6.39×10^{-4}
Ntus	30 October 2003	2.78×10^{-4}	6.98×10^{-4}	1.40×10^{-3}
Ankr	31 October 2003	1.20×10^{-4}	2.34×10^{-4}	3.31×10^{-4}
Artu	31 October 2003	2.67×10^{-4}	8.72×10^{-4}	8.36×10^{-4}

very similar and the differences between the estimates are very small. These two weighting options reduces non-ionospheric irregularities better compared to the $w1^m(n)$ weighting function.

[22] The normalized differences between the estimates are also calculated in equations (38), (39) and (40) as follows

$$Err_{15} = \frac{\sum_{n=1}^{N} |\tilde{\mathbf{x}}_{w3}(n) - \tilde{\mathbf{x}}_{w2}(n)|^2}{\sum_{n=1}^{N} |\tilde{\mathbf{x}}_{w2}(n)|^2} \qquad (38)$$

$$Err_{16} = \frac{\sum_{n=1}^{N} |\tilde{\mathbf{x}}_{w2}(n) - \tilde{\mathbf{x}}_{w1}(n)|^2}{\sum_{n=1}^{N} |\tilde{\mathbf{x}}_{w2}(n)|^2} \qquad (39)$$

$$Err_{17} = \frac{\sum_{n=1}^{N} |\tilde{\mathbf{x}}_{w3}(n) - \tilde{\mathbf{x}}_{w1}(n)|^2}{\sum_{n=1}^{N} |\tilde{\mathbf{x}}_{w2}(n)|^2} \qquad (40)$$

where n denotes the time index of the vectors and N is the total number of estimates. The normalized TEC estimate differences Err_{15}, Err_{16} and Err_{17} are in listed in Table 5 for various stations and for both disturbed and quiet days of October 2003. In Table 5, Err_{15} values are smaller than Err_{16} and Err_{17} which means that regularized estimates due to applying second or third weighting functions are very similar to each other. The TEC estimates when the first weighting function is applied are slightly different compared to those due to $w2^m(n)$, and $w3^m(n)$. It is seen in Figure 5 that $\tilde{\mathbf{x}}_{w2}$ and $\tilde{\mathbf{x}}_{w3}$ are smoother than $\tilde{\mathbf{x}}_{w1}$. The second and third weighting functions, due to their smooth transitions in elevation angles result in smoother TEC estimates, reducing non-ionospheric noise effects. Therefore the second or third weighting functions might be better options to be used in Reg-Est method.

7. Conclusion

[23] Reg-Est is an efficient and robust technique for estimating TEC with 30 s time resolution. Reg-Est produces reliable TEC estimates for both quiet and disturbed days of the ionosphere and for all stations in mid-latitude, high latitude and equatorial regions. In this study, various parameters of Reg-Est are investigated in detail and alternatives where applicable are selected for better TEC estimation. In

this paper, the ambiguity of how to include the differential code biases into the TEC computation is resolved by considering possible alternatives given in the literature and applying them separately through Reg-Est algorithm. After a detail investigation of the normalized differences with the IGS TEC estimates over various days and stations, it is decided that it is a better choice to include the differential code biases in the computation of $STEC$ as given in equations (14) and (25).

[24] In previous studies of Reg-Est method, only pseudo-range measurements were used as input. In this paper, an alternative technique is developed to compute the TEC from phase-corrected $VTEC$. The TEC estimation results from both pseudo-range and phase-corrected TEC are very close but TEC estimations from phase-corrected input $VTEC$ are less noisy. Thus in the future, both absolute TEC and phase-corrected TEC can be used in Reg-Est.

[25] Ionospheric shell height is another parameter used in Reg-Est in the preprocessing of $VTEC$ from individual satellites in view. In this paper, different ionospheric shell height values are tried in Reg-Est and the TEC estimates are compared. It is observed that Reg-Est is practically independent of the choice of ionospheric height.

[26] Weighting function helps to reduce the multipath effect in the measurements of satellites which are at low elevation angles. In this study, three possible alternatives for weighting functions are tried in the Reg-Est and the weighting function in equation (36), that reduces the non-ionospheric effects best, is selected.

[27] As a result, all the parameters of Reg-Est is investigated and the optimum parameter set is selected. The measurement input data set is enlarged to include carrier phase data. It is also shown that the Reg-Est TEC estimates are in very good agreement with those of IGS analysis centers, especially, with CODE and JPL.

References

Arikan, F., C. B. Erol, and O. Arikan (2003), Regularized estimation of vertical electron content from Global Positioning System data, *J. Geophys. Res.*, 109(A12), 1469, doi:10.1029/2003JA009605.

Arikan, F., C. B. Erol, and O. Arikan (2004), Regularized estimation of vertical total electron content from GPS data for a desired time period, *Radio Sci.*, 39, RS6012, doi:10.1029/2004RS003061.

Arikan, F., O. Arikan, and C. B. Erol (2007), Regularized estimation of TEC from GPS data for certain mid-latitude stations and comparison with the IRI model, *Adv. in Space Res.*, 39, 867–874, doi:10.1016/j.asr.2007.01.082.

Bilitza, D. (2001), IRI 2000, *Radio Sci.*, 36(2), 261–276.

Budden, K. G. (1985),*The Propagation of Radio Waves:The Theory of Radio Waves of Low Power in the Ionosphere and Magnetosphere*, Cambridge Univ. Press, Cambridge.

Feltens, J., and N. Jakowski (2002), International GPS Service (IGS) Ionosphere Working Group Activity, SCAR Report No 21, SCAR Working Group on Geodesy and Geographic Information, Russia 18–20 July.

Foster, J. C., and W. Rideout (2005), Midlatitude TEC enhancements during the October 2003 superstorm, *Geophys. Res. Lett.*, 32, L12S04, doi:10.1029/2004GL021719.

Hargreaves, J. K. (1992), *The Solar-Terrestrial Environment*, Cambridge Univ. Press, Cambridge.

Jakowski, N., E. Sardon, E. Engler, A. Jungstand, and D. Klahn (1996), Relationships between GPS-signal propagation errors and EISCAT observations, *Ann. Geophysicae*, 14, 1429–1436.

Komjathy, A. (1997), Global Ionospheric Total Electron Content Mapping Using the Global Positioning System, Ph.D. Thesis, Dept. of Geodesy

and Geomatics Engineering Technical Report No. 188, Univ. of New Brunswick, Fredericton, New Brunswick, Canada.

Komjathy, A., and R. Langley (1996), An assesment of predicted and measured ionospheric total electron content using a regional GPS network, paper presented at Nat. Tech. Meet., Inst. of Nav., Santa Monica, CA 22–24 January.

Kunitsyn, V. E., and E. D. Tereshchenko (2003), *Ionospheric Tomography*, Springer, Berlin.

Lanyi, G. E., and T. Roth (1988), A comparison of mapped and measured total ionospheric electron content usin global positioning system and beacon satellite observations, *Radio Sci.*, *23*, 483–492.

Leick, A. (2004), *GPS Satellite Surveying*, 3rd ed., John Wiley and Sons Inc., New Jersey.

Liao, X. (2000), Carrier phase based ionosphere recovery over a regional area GPS network, M.Sc. Thesis, Univ. of Calgary, Canada.

Lin, C. H., A. D. Richmond, J. Y. Liu, H. C. Yeh, L. J. Paxton, G. Lu, H. F. Tsai, and S.-Y. Su (2005), Large-scale variations of the low-latitude ionosphere during the October-November 2003 superstorm: Observational results, *J. Geophys. Res.*, *110*, A09S28, doi:10.1029/2004JA010900.

Ma, G., and T. Maruyama (2003), Derivation of TEC and estimation of instrumental biases from GEONET in Japan, *Ann. Geophys.*, *21*, 2083–2093.

Makalea, J. J., M. C. Kelley, J. J. Sojka, X. Pi, and A. J. Manucci (2001), GPS normalization and preliminary modeling results of total electron content during midlatitude space weather event, *Radio Sci.*, *36*, 356–361.

Manucci, A. J., B. D. Wilson, D. N. Yuan, C. H. Ho, U. J. Lindqwister, and T. F. Runge (1998), A global mapping technique for GPS-derived ionospheric total electron content measurements., *Radio Sci.*, *33*, 565–582.

Mitchell, C. N., L. Alfonsi, G. De Franceschi, M. Lester, V. Romano, and A. W. Wernik (2005), GPS TEC and scintillation measurements from the polar ionosphere during the October 2003 storm, *Geophys. Res. Lett.*, *32*, L12S03, doi:10.1029/2004GL021644.

Nayir, H. (2007), Ionospheric Total Electron Content Estimation Using GPS Signals (in Turkish), M.Sc. Thesis, Hacettepe Univ., Ankara, Turkey.

Otsuka, Y., T. Ogawa, A. Saito, T. Tsugawa, S. Fukao, and S. Miyazaki (2002), A new technique for mapping of total electron content using GPS network in Japan, *Earth Planets Space*, *54*, 63–70.

Schaer, S. (1999), Mapping and predicting the Earth's ionosphere using the global positioning system, Ph.D. Thesis, Univ. of Berne, Berne, Switzerland.

Warnant, R. (1997), Reliability of the TEC computed using GPS measurements - The problem of hardware biases, *Acta Geod. Geoph. Hung.*, *32*(3–4), 451–459.

Yizengaw, E., M. B. Moldwin, P. L. Dyson, and T. J. Immel (2005), Southern Hemisphere ionosphere and plasmasphere response to the interplanetary shock event of 29–31 October 2003, *J. Geophys. Res.*, *110*, A09S30, doi:10.1029/2004JA010920.

————————————

F. Arikan, Department of Electrical and Electronics Engineering, Hacettepe University, Beytepe, 06532, Ankara, Turkey. (arikan@hacettepe. edu.tr)

O. Arikan, Department of Electrical and Electronics Engineering, Bilkent University, Bilkent, 06533, Ankara,Turkey. (oarikan@ee.bilkent.edu.tr)

C. B. Erol, TUBITAK, UEKAE, Kavaklidere, 06100, Ankara,Turkey. (cemil.erol@iltaren.tubitak.gov.tr)

H. Nayir, Department of Microwave and System Technologies, Aselsan Inc., Yenimahalle, Ankara, 06370, Turkey. (hnayir@mst.aselsan.com.tr)